Theoretical optoelectronic analysis of intermediate-band photovoltaic material based on $ZnY_{1-x}O_x$ (Y = S, Se, Te) semiconductors by first-principles calculations*

Wu Kong-Ping(吴孔平)[a)b)†], Gu Shu-Lin(顾书林)[b)‡], Ye Jian-Dong(叶建东)[b)], Tang Kun(汤 琨)[c)], Zhu Shun-Ming(朱顺明)[b)], Zhou Meng-Ran(周孟然)[a)], Huang You-Rui(黄友锐)[a)], Zhang Rong(张 荣)[b)], and Zheng You-Dou(郑有炓)[b)]

[a)] *School of Electrical and Information Engineering, Anhui University of Science and Technology, Huainan* 232001, *China*
[b)] *Nanjing National Laboratory of Microstructures, School of Electronic Science and Engineering, Nanjing University, Nanjing* 210093, *China*
[c)] *Data Storage Institute, A*STAR, Singapore* 117608, *Singapore*

(Received 25 February 2013; revised manuscript received 31 March 2013)

The structural, energetic, and electronic properties of lattice highly mismatched $ZnY_{1-x}O_x$ (Y = S, Se, Te) ternary alloys with dilute O concentrations are calculated from first principles within the density functional theory. We demonstrate the formation of an isolated intermediate electronic band structure through diluted O-substitute in zinc-blende ZnY (Y = S, Se, Te) at octahedral sites in a semiconductor by the calculations of density of states (DOS), leading to a significant absorption below the band gap of the parent semiconductor and an enhancement of the optical absorption in the whole energy range of the solar spectrum. It is found that the intermediate band states should be described as a result of the coupling between impurity O 2p states with the conduction band states. Moreover, the intermediate bands (IBs) in ZnTeO show high stabilization with the change of O concentration resulting from the largest electronegativity difference between O and Te compared with in the other ZnSO and ZnSeO.

Keywords: intermediate band (IB), electronic band structure, optical properties, electronegativity

PACS: 71.20.–b, 71.15.Mb, 78.20.Ci, 74.25.Gz **DOI:** 10.1088/1674-1056/22/10/107103

1. Introduction

In the quest for more efficient photovoltaics, a new proposal was made recently,[1] in which a partially filled band is introduced inside the band gap of a semiconductor so that the promotion of an electron from the valence band to the conduction band may be produced not only with a photon of band gap energy or higher, but also by absorbing two photons of lower energy (Fig. 1). The process involves a partially occupied intermediate band (IB) that serves as a "stepping stone" for the transition, which leads to an increase in photocurrent without reducing the photovoltage. A maximum ideal efficiency of 63.1% can thus be attained, much higher than the well-known Queisser limit of (single junction) normal cells (40.7%). There is thus interest in finding material compositions able to produce the desired electronic structure.

Recently a new class of semiconductors has emerged, whose fundamental properties are dramatically modified through substituting a relatively small fraction of host atoms with an element of very different electronegativity, the so-called highly mismatched alloys (HMAs). III–V and II–VI alloys in which group V and VI anions are replaced with the isovalent N[2] and O,[3,4] respectively are the well-known examples of the HMAs. The band structure of HMA is well described by the band anticrossing (BAC) model[5] which has shown that some of the dilute nitrides or oxides exhibit unusual energy band structures each with a narrow band of states located in the band gap of the host material indicating that such HMAs could be used for multiband solar cells. Especially, López reported how the tailoring of the electronic band structure of highly mismatched alloys could be used to design semiconductor materials for specific device applications. They were able to successfully realize an intermediate band photovoltaic device by N-doped GaAs alloys.[6]

The II–VI semiconductors have technological applications in fabricating optoelectronic devices. One of the salient features of the HMAs is that a replacement of the anion atoms with isoelectronic atoms with very different electronegativity values results in the formation of localized electronic states. As is well known, the group VI elements have electronegativity values ranging from 2.08 to 3.47 (from Te up to O) using the Pauling scale.[7] At one extreme, S and Se are very similar,

*Project supported by the State Key Program for Basic Research of China (Grant No. 2011CB302003), the Project of High Technology Research and Development Program of China (Grant No. 2007AA03Z404), the National Natural Science Foundation of China (Grant Nos. 60990312, 61274058, 61025020, and 61073101), and the Natural Science Foundation of Anhui Province, China (Grant No. 1208085QF116).

†Corresponding author. E-mail: kpwu@aust.edu.cn
‡Corresponding author. E-mail: slgu@nju.edu.cn

© 2013 Chinese Physical Society and IOP Publishing Ltd

with only a 0.1 difference in electronegativity, and on the other hand, Te and O differ by 1.39. Se and Te have a moderate electronegativity difference of 0.3. The BAC model suggests that the strength of the anticrossing interaction in HMA depends on the electronegativity mismatch. Therefore, one can anticipate it to be particularly pronounced in group II–O_x–VI_{1-x} alloys in view of the very highly electronegative O atoms substituting the significantly more metallic column VI elements. The new II–VI alloy IB materials have technological potentials for photovoltaic applications. Efforts to improve the efficiency of solar cells have led to extensive experimental and theoretical studies of new materials and cell designs.[8–10]

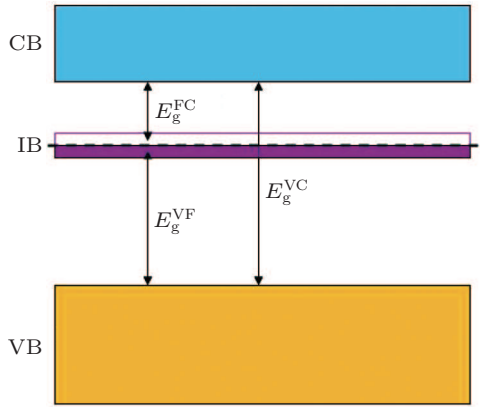


Fig. 1. (color online) Band diagram of an IB solar cell, showing the bandgap E_g^{VC}, the sub-bandgaps E_g^{FC} and E_g^{VF}, as well as the conduction band (CB), intermediate band (IB), and valence band (VB).

While the band gaps of IB-materials are often used as an evaluation criterion, the issue with shape and overlap of the absorption coefficients has not been paid much attention so far. In this work, a theoretical study is presented on the electronic and optical properties of the highly mismatched ternary $ZnY_{1-x}O_x$ (Y = S, Se, Te) alloys in the framework of density functional theory (DFT). The calculated band structures and absorption coefficients indicate that the highly mismatched ternary $ZnY_{1-x}O_x$ (Y = S, Se, Te) compound materials have direct band gaps and are excellent new photovoltaic materials. In particular, the characteristics and positions of the electronic states formed in all cases are examined to anticipate the possible formation of an intermediate-band photovoltaic material with the desired properties. In addition, optical properties of a potential intermediate-band material close to the experimental conditions are computed. The improvement on the absorption coefficient across the solar spectrum produced by the IB is verified.

2. Method

Band structure and total energy calculations using first principles density functional theory (DFT) were performed using the CASTEP program[11–13] with the plane wave pseudopotential approach. The generalized gradient approximation (GGA) was employed to simulate the electron exchange–correlation energy. The energy cutoff established for the basis set was 285 eV. Projector augmented wave (PAW) potentials were used to represent the inert core electrons. Density functional theory (DFT) calculations were carried out to obtain electronic and optical properties of compounds based on $ZnY_{1-x}O_x$ (Y = S, Se, Te) alloys at concentrations close to those of the experiment.[14,15] Three different supercells of conventional Zn_4Y_4 (Y = S, Se, Te) zinc-blende unit cell structure were considered to include the O implantation: $1\times1\times2$ ($Zn_8Y_7O_1$), $2\times1\times2$ ($Zn_{16}Y_{15}O_1$), and $2\times2\times2$ ($Zn_{32}Y_{31}O_1$) (Y = S, Se, Te) where S, Se, and Te atoms were replaced by O. For all calculations, the experimental lattice constants of zinc-blende ZnS, ZnSe, and ZnTe are assumed to be 5.41 Å, 5.67 Å, and 6.10 Å, respectively. The samplings used to describe the Brillouin zone corresponding to the compounds derived from the $1\times1\times2$, $2\times1\times2$, and $2\times2\times2$ supercells were centered $6\times6\times6$, $4\times4\times4$, and $2\times2\times2$ grids, respectively. In the optimization process, the energy change, maximum force, maximum stress, and maximum displacement tolerances were set to be 2×10^{-5} eV/atom, 0.05 eV/Å, 0.1 GPa, and 0.002 Å, respectively. In addition, both lattice constants and atomic positions were optimized whenever available. The optical behaviors of the materials were characterized by their absorption coefficients derived from the dielectric function. The imaginary part of the dielectric function was obtained by the sum over independent transitions between Kohn–Sham states.

3. Results and discussion

3.1. Cohesive energy and electronic structure

The electronic band structures of $ZnY_{1-x}O_x$ (Y = S, Se, Te) zinc-blende supercell structure are shown in Figs. 2(a)–2(c), respectively. The band structures of zinc-blende ZnY, Zn_8Y_7O, $Zn_{16}Y_{15}O$, and $Zn_{32}Y_{31}O$ (Y = S, Se, Te) were obtained along the *G–F–Q–Z–G* path in the first Brillouin zone. Similar results have been found in Yu *et al.*'s work.[16] From Fig. 2, the band gaps of zinc-blende ZnS, ZnSe, and ZnTe are about 2.11, 1.36, and 1.26 eV, respectively, and it is interesting to note that the values of the experimentally measured band gap are 3.6, 2.7, 2.25 eV.[17,18] Such an underestimation is explained by the DFT limitations, as the discontinuity in the exchange correlation potential has not been taken into account. However, these results are advisable for the qualitative analysis and do not affect the accuracy of comparing the relevant properties of crystals (band structure, density of states, and absorbed spectra).[19]

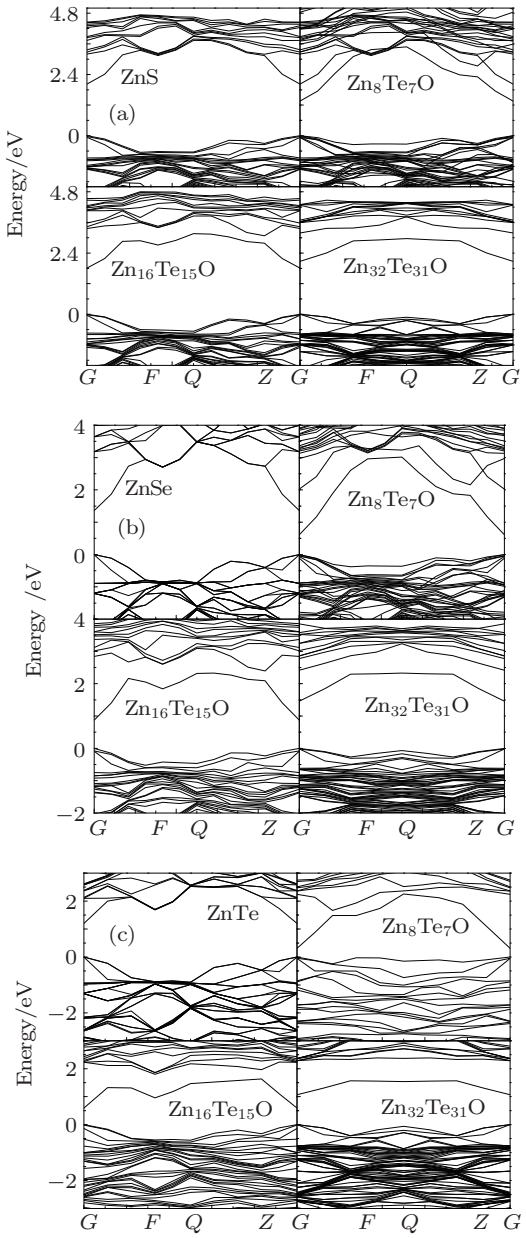


Fig. 2. Band structures obtained for the relaxed ZnY_{1-x}:O_x (Y = S, Se, Te) compound corresponding to panels (a), (b), and (c).

As shown in $ZnTe_{1-x}O_x$ band structure (Fig. 2(c)), the energy level related to O impurities appears in the band gap and the value of band gap is also found to decrease resulting from the increase of O composition. In addition, from the view of band structure, $Zn_{32}Te_{31}O$, $Zn_{16}Te_{15}O$, and Zn_8Te_7O are direct band gap semiconductors, and the calculated values of the band gap are about 0.31, 0.59, and 1.06 eV, respectively, which are much lower than the band gap of zinc-blende ZnTe (1.26 eV). Besides, for a small O concentration, the energy level related to O impurities is completely separated from the CB, and the energy levels in CB become increasingly flat. But for a heavy concentration of O in $ZnY_{1-x}O_x$ (Y = S, Se, Te), the energy level related to O impurities moves towards the CB, and it evolves to connecting the CB even more. For $ZnSe_{1-x}O_x$ (Fig. 2(b)), these results are very similar to those of $ZnTe_{1-x}O_x$, while for $ZnS_{1-x}O_x$ (Fig. 2(a)), the trend of the energy level related to O moving towards the conduction band is out rapidly compared with for $ZnTe_{1-x}O_x$ and $ZnSe_{1-x}O_x$. It must be due to a small electronegativity difference between O and S. Specifically, Te and O differ by 1.39. Se and O have an electronegativity difference of 1.1. S and O have an electronegativity difference of about 0.99. The BAC model suggests that the strength of the anticrossing interaction in HMAs depends on the electronegativity mismatch.

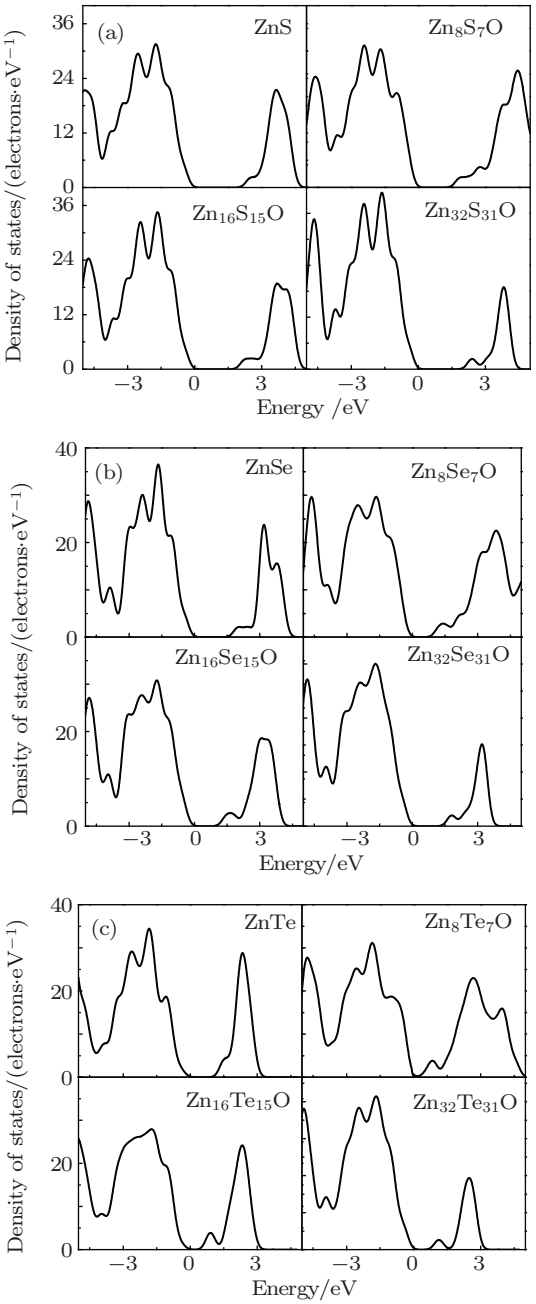


Fig. 3. Total DOSs calculated for the ZnY_{1-x}:O_x (Y = S, Se, Te) compound corresponding to panels (a), (b), and (c). The Fermi level is set to be $E = 0$.

To explain the formation of the IB, the systems we are interested in could be visualized in our study as a substitution of single impurity atom (O) in the zinc-blende crystal structure of

the parent semiconductors ZnY (Y = S, Se, Te). Figures 3(a)–3(c) show the densities of states (DOSs) of ZnY_{1-x}O$_x$ (Y = S, Se, Te) for x = 12.5%, 6.25%, and 3.125% respectively; they correspond to O atoms in the 16, 32, 64-atom supercells. With the decrease in O concentration, an IB is formed inside the ZnY (Y = S, Se, Te) band gap. In particular, the IB is completely separated from the CB for x about 3.125% O concentration in ZnTe$_{1-x}$O$_x$ in Fig. 3(c). We notice that the width of the IB increases and the IB becomes connected with the CB with O concentration x increasing. The same results happen to ZnSe$_{1-x}$O$_x$ and ZnS$_{1-x}$O$_x$ in Figs. 3(b) and 3(a) respectively; in such a heavy O concentration, it is very difficult to form IB inside the ZnS and ZnSe band gap. For a solar cell application, such a system is no longer useful because the electron in the CB will be relaxed to the IB states by phonon emission.

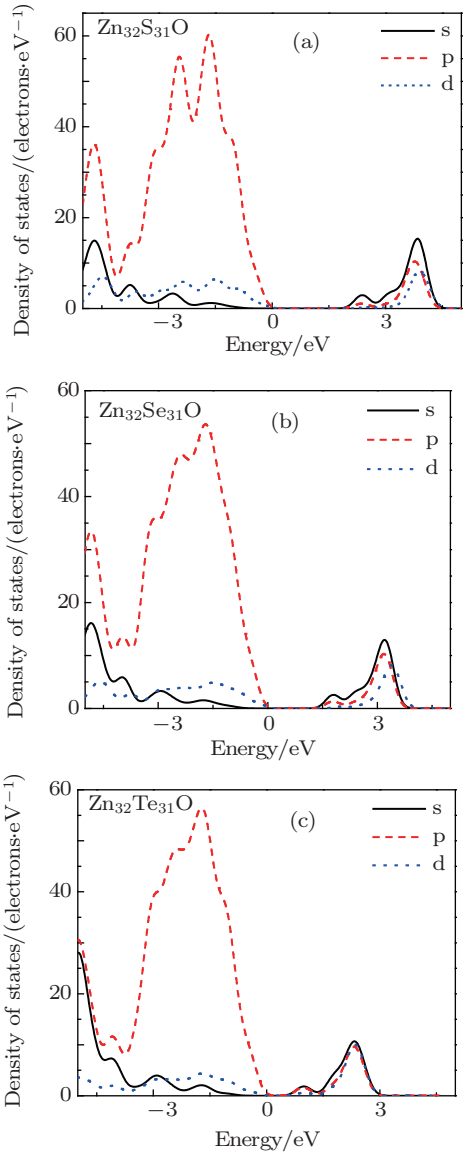


Fig. 4. (color online) Partial DOS O 2p and Zn 3d4s curves obtained with GGA calculations for ZnY_{1-x}:O$_x$ (Y = S, Se, Te) compound (a) ZnS$_{1-x}$:O$_x$, (b) ZnSe$_{1-x}$:O$_x$, and (c) ZnTe$_{1-x}$:O$_x$. The Fermi level is set to $E = 0$.

These results for ZnY_{1-x}O$_x$ (Y = S, Se, Te) also indicate possible IB properties, which could also imply interesting applications in solar cell materials and cell designs. Since these features depend strongly on the degree of electronic correlation, for a better description of formation of the IB the partial DOS is calculated by GGA for ZnY_{1-x}O$_x$ (Y = S, Se, Te). These are shown in Figs. 4(a)–4(c). For Zn$_{32}$Te$_{31}$O in Fig. 4(c), the IB is formed in the energy region between 0.7 eV and 1.35 eV, which is mainly composed of the O 2p band and Zn 3d band with smaller mixing of Zn 4s bands. For Zn$_{32}$S$_{31}$O and Zn$_{32}$Se$_{31}$O in Figs. 4(a) and 4(b), CB mainly contains contributions from the O 2p band and Zn 3d4s band, indicating that the hybridization takes place between these states and also that the formation of IB will involve both O 2p and Zn 3d4s states. If O concentration decreases in the whole crystal, it could give rise to an IB instead of a state. The characteristics of the interactions between the atoms and the overlapping of the orbitals in the suitable directions will determine the possibility of the narrow and isolated band formation.

From Fig. 3 the IB is formed inside the ZnY (Y = S, Se, Te) band gap with the decrease in O concentration. We notice that the IB is completely separated from the CB for x about 3.125% O concentration in ZnTe$_{1-x}$O$_x$ in Fig. 3(c), while IB is still connected with the CB for x about 3.125% O concentration in ZnSe$_{1-x}$O$_x$ or ZnS$_{1-x}$O$_x$ in Figs. 3(a) and 3(b). Therefore, the smaller O concentrations in Zn$_{48}$S$_{47}$O are studied. Total DOS and partial DOS for O 2p and Zn 3d4s curves in Zn$_{48}$S$_{47}$O$_x$ compound are shown in Figs. 5(a) and 5(b), respectively. The expected IB is completely separated from the CB for x about 2.08% O concentration in ZnS$_{1-x}$O$_x$ in Fig. 5(a). Figure 5(b) shows that the IB is mainly composed of Zn 4d band with smaller mixing of the O 2p band.

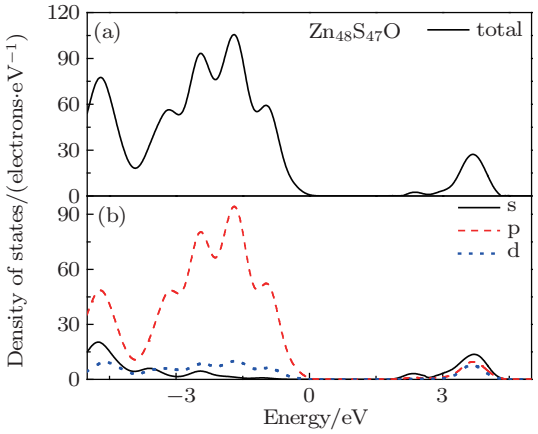


Fig. 5. (color online) Total DOS (a) and partial DOS (b) O 2p and Zn 3d4s curves obtained with GGA calculations for Zn$_{48}$S$_{47}$O$_x$ compound. The Fermi level is set to be $E = 0$.

It is interesting that the IB is completely separated from the CB for x about 3.125% O concentration in ZnTe$_{1-x}$O$_x$ in Fig. 3(c) and the IB is completely separated from the CB for x about 2.08% O concentration in ZnS$_{1-x}$O$_x$ in Fig. 5(a).

These different results could be attributed to the small difference in the electronegativity between S and O compared with between Te and O, and the difference in ionicity between ZnS and ZnTe.

3.2. Optical properties

Band gaps obtained from Figs. 2(a)–2(c) are averaged gaps, and so they may not be totally representative of optical properties, as it is the minimum band gap, the one that will determine the onset of partial absorption coefficient. Therefore, the study of optical properties will give much more information about that subject.

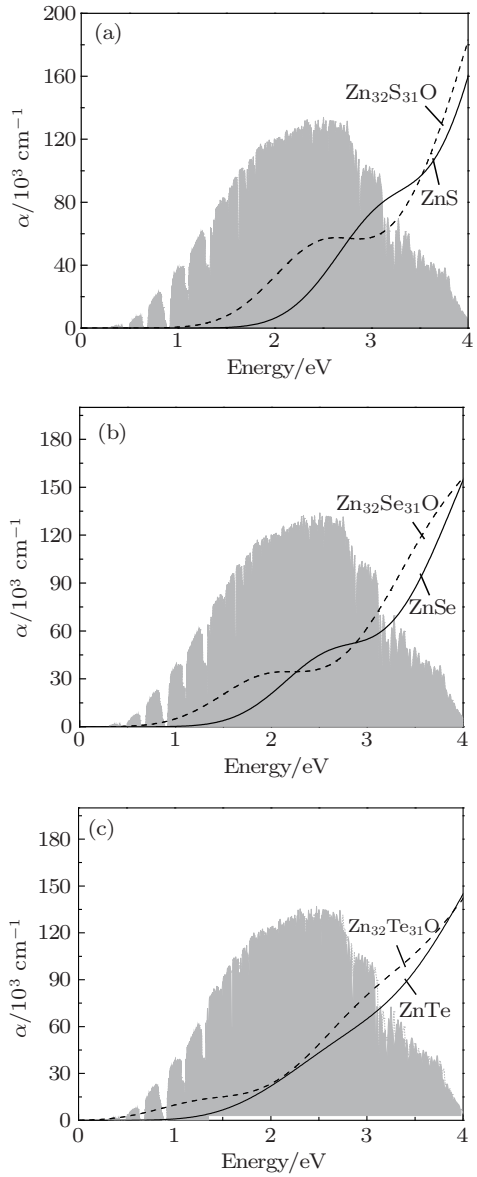


Fig. 6. Optical absorption coefficients calculated (a), (b), and (c) for ZnY and $Zn_{32}Y_{31}O$ (Y = S, Se, Te) compounds, respectively. The solar spectrum AM 1.5G (in arb. units) is included as a reference in the background.

Now, we come to first focus on the absorption coefficients obtained for $Zn_{32}Y_{31}O$ (Y = S, Se, Te). Figures 6(a)–6(c) show the absorption coefficients of $Zn_{32}Y_{31}O$ (Y = S, Se, Te) compared with those of the pure semiconductors ZnY (Y = S, Se, Te). The solar spectrum is displayed as a background to show the enhancement in absorption due to the IB in the main part of the solar spectrum.

It should be noticed that the absorption property curves for α values of ZnY (Y = S, Se, Te) go to zero at 1.7, 1.2, and 0.9 eV respectively, while the absorption coefficients of $Zn_{32}Y_{31}O$ (Y = S, Se, Te) start at around 1.1, 0.7, and 0.3 eV respectively. The energy band structures are dramatically changed, resulting from the larger electronegativity O involved in ZnY (Y = S, Se, Te), which makes the band gap smaller or the IB formed in band gap of ZnY (Y = S, Se, Te).

In addition to the main absorption edge at approximately 2.5 eV for $Zn_{32}Te_{31}O$ in Fig. 6(c), two new main features appear compared with for ZnTe: (i) a distinct shoulder or step starting at approximately 1.9 eV, which can be due to transition VB→IB or VB→CB, and (ii) a broad absorption that starts at rather low energy, possibly around 0.3 eV, and increases steadily until meeting the other feature at approximately 1.9 eV. This second characteristic may be related to the transition IB→CB.

It is known that the dielectric function is mainly related to the electronic response. Acquaintance of optical properties is of great importance in the designs and analyses of optoelectronic devices such as light sources and detectors. These properties are described for a medium by the complex dielectric function[20]

$$\varepsilon(\omega) = \varepsilon_1(\omega) + \mathrm{i}\varepsilon_2(\omega),$$

where the two parts of the dielectric function, real (ε_1) and imaginary (ε_2), are related by the Kramers–Kronig relation. Figure 7 shows the spectral variations of real (ε_1) and imaginary (ε_2) calculated theoretically based on DFT for ZnTe and $Zn_{32}Te_{31}O$.

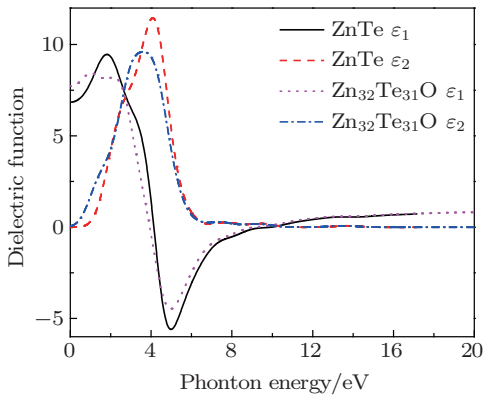


Fig. 7. (color online) Dielectric functions of ZnTe and $Zn_{32}Te_{31}O$.

The imaginary component of the dielectric constant and its different contributions are examined (see Fig. 7) to verify the role that the IB plays in the absorption enhancement, according to the close relationship between the optical properties and the dielectric constant.[20] It can be seen that the main

contribution below 3.5 eV is related to the IB levels. Apart from the interband transitions, which are not relevant to photo conversion, there is a peak at 1.3 eV resulting from electronic transition from the minority IB to the CB. All these are in consistence with the peak positions in absorption in Fig. 6(c).

We briefly discuss the relationship between the complex dielectric function and absorption spectrum. The imaginary component of the dielectric constant and its different contributions are examined to verify the role that the IB plays in the absorption enhancement. Owing to this electronic structure feature, these materials will allow the absorption of photons with energy below the band gap, in addition to the normal light absorption of a semiconductor. Moreover, these zinc-blende ZnY (Y = S, Se, Te) derivatives, for which the technology to grow them into thin films is already known, seem to be promising systems for developing more efficient novel optoelectronic devices.

In addition, calculations of the electronic structure are affected by the well-known band gap underestimation characteristic of the DFT method. However, this underestimation does not severely affect the main results of the general shield carried out in this work in the presence or absence of IB upon substitution of species at the cation sublattices. We have not deliberately corrected the values obtained for the band gaps, a common practice in studies of electronic structure based on DFT calculations. Although the absolute positions of the eventual IB and the absorption energy are thus not accurately calculated without further corrections, we can conclude that whether the intermediate states exist is related to the improving optical properties, while avoiding certain arbitrariness related with the shifts to be introduced to correct the band gaps.

4. Conclusions

In this paper, through first-principles calculations we obtain the structural, electronic, and optical properties of new diluted O-substitute in zinc-blende ZnY (Y = S, Se, Te) supercell structure presenting a narrow intermediate band isolated from the VB and the CB of the host semiconductor. The computed optical absorptions of these compounds compared with the corresponding un-doped semiconductor show each possess a significant absorption below the band gap of the parent semiconductor and an enhancement of the optical absorption in the whole energy range of the visible region. We demonstrate the formation of an isolated intermediate electronic band structure through diluted O-substitute in zinc-blende ZnY (Y = S, Se, Te) at octahedral sites in a semiconductor by DOS calculations, leading to an enhancement of the absorption coefficient in both infrared and visible ranges of the solar spectrum. The IBs in ZnTeO compared with in other ZnSO and ZnSeO show high stabilization with the change of O concentration resulting from the largest electronegativity difference between O and Te. The electronic structure features like those of ZnYO (Y = S, Se, Te) could be used for developing a new next-generation photovoltaic cell. The extraordinary band engineering potential in high mismatched alloys has advantages for photovoltaic, thermoelectric, and optoelectronic applications.

References

[1] Luque A and Martí A 1997 *Phys. Rev. Lett.* **78** 5014
[2] Yu K M, Walukiewicz W, Beeman J W, Scarpulla M A, Dubon O, Pillai M R and Aziz M 2002 *Appl. Phys. Lett.* **80** 3958
[3] Yu K M, Walukiewicz W, Wu J, Beeman J W, Ager J W, Haller E E, Miotkowski I, Ramdas A K and Becla P 2002 *Appl. Phys. Lett.* **80** 1571
[4] Tanaka T, Miyabara M, Nagao Y, Saito K, Guo Q, Nishio M, Yu K M and Walukiewicz W 2013 *Appl. Phys. Lett.* **102** 052111
[5] Walukiewicz W, Shan W, Yu K M, Ager J W, Haller E E, Miotkowski I, Seong M J, Alawadhi H and Ramdas A K 2000 *Phys. Rev. Lett.* **85** 1552
[6] López N, Reichertz L A, Yu K M, Campman K and Walukiewicz W 2011 *Phys. Rev. Lett.* **106** 028701
[7] Gordy W 1946 *Phys. Rev.* **69** 604
[8] Wang W M, Lin A S and Phillips J D 2010 *Appl. Phys. Lett.* **95** 011103
[9] Dong A, Wang F, Daulton T L and Buhro W E 2007 *Nano Lett.* **7** 1308
[10] Lee B and Wang L W 2010 *Appl. Phys. Lett.* **96** 071903
[11] Zhao L, Lu P F, Yu Z Y, Guo X T, Shen Y, Ye H, Yuan G F and Zhang L 2010 *J. Appl. Phys.* **108** 113924
[12] Zhu F, Dong S and Cheng G 2011 *Chin. Phys. B* **20** 077103
[13] Lü B, Zhou X, Linghu R F, Wang X L and Yang X D 2011 *Chin. Phys. B* **20** 036104
[14] Nabetani Y, Mukawa T, Okuno T, Ito Y, Kato T and Matsumoto T 2003 *Mater. Sci. Semicond. Process.* **6** 343
[15] Wang W, Lin A S and Phillips J D 2009 *Appl. Phys. Lett.* **95** 011103
[16] Yu Q H, Jin L and Zhou C G 2011 *Sol. Energy Mater. & Sol. C* **95** 2322
[17] Nabetani Y, Okuno T, Aoki K, Kato T, Matsumoto T and T Hirai 2006 *Phys. Stat. Sol. (c)* **3** 1078
[18] Nabetani1 Y, Ito Y, Kamisawa K, Kato T, Matsumoto T and T Hirai 2006 *Phys. Stat. Sol. (c)* **3** 1082
[19] Umebayashi T, Yamaki T, Itoh H and Asai K 2002 *J. Phys. Chem. Solids* **63** 1909
[20] Saha S, Sinha T P and Mookerjee A 2000 *Phys. Rev. B* **62** 8828